AFRL-RV-PS-
TR-2023-0122 Vol 2

AFRL-RV-PS-
TR-2023-0122 Vol 2

NOISE MEASUREMENTS AND CURRENT DRIVER IMPROVEMENTS FOR AN ATOM INTERFEROMETER GYROSCOPE

M. M. Beydler, et al.

**Department of Physics University of Virginia
University of Virginia
1001 N Emmet Street
Charlottesville, VA 22903-4833**

08 October 2023

Final Report

**AIR FORCE RESEARCH LABORATORY
Space Vehicles Directorate
3550 Aberdeen Ave SE
AIR FORCE MATERIEL COMMAND
KIRTLAND AIR FORCE BASE, NM 87117-5776**

REPORT DOCUMENTATION PAGE

Form Approved
OMB No. 0704-0188

1. REPORT DATE *(DD-MM-YYYY)*
08-10-2023

2. REPORT TYPE
Final Report

3. DATES COVERED *(From - To)*
17 May 2019 to 08 Oct 2023

4. TITLE AND SUBTITLE
Noise Measurements and current Driver Improvements for an Atom Interferometer Gyroscope

5a. CONTRACT NUMBER
FA9453-19-1-0007

5b. GRANT NUMBER

5c. PROGRAM ELEMENT NUMBER
61101E (DARPA)

6. AUTHOR(S)
M. M. Beydler, E. R. Moan, and C. A. Sackett

5d. PROJECT NUMBER
1000

5e. TASK NUMBER
EF134910

5f. WORK UNIT NUMBER
V1NN

7. PERFORMING ORGANIZATION NAME(S) AND ADDRESS(ES)
Department of Physics University of Virginia
University of Virginia
1001 N Emmet Street
Charlottesville, VA 22903-4833

8. PERFORMING ORGANIZATION REPORT NUMBER

9. SPONSORING / MONITORING AGENCY NAME(S) AND ADDRESS(ES)
Air Force Research Laboratory
Space Vehicles Directorate
3550 Aberdeen Avenue SE
Kirtland AFB, NM 87117-5776

10. SPONSOR/MONITOR'S ACRONYM(S)
AFRL/RVBYT

11. SPONSOR/MONITOR'S REPORT NUMBER(S)
AFRL-RV-PS-TR-2023-0122 Vol 2

12. DISTRIBUTION / AVAILABILITY STATEMENT
Approved for public release; distribution is unlimited (AFRL-2023-5607 dtd 06 Nov 2023).

13. SUPPLEMENTARY NOTES

14. ABSTRACT
We present noise measurements for our Bragg interferometer gyroscope in a time-orbiting potential trap. We obtain an Allan deviation plot that demonstrates averaging improvement as $1/\sqrt{T}$ up to integration times T of 2.5 h. However, it exhibits an unexpected short term noise level of approximately 9 rad/$\sqrt{\text{Hz}}$. We attribute this primarily to real phase noise in the interferometer caused by fluctuations in the trap drive current. We have developed and constructed new high-bandwidth current amplifiers that we anticipate will improve performance.

15. SUBJECT TERMS
quantum, gyroscope, atom, atomic, interferometer, interferometry, Bose-Einstein condensate, BEC, time-orbiting potential, magnetic trap, trapped atoms

16. SECURITY CLASSIFICATION OF:			**17. LIMITATION OF ABSTRACT**	**18. NUMBER OF PAGES**	**19a. NAME OF RESPONSIBLE PERSON**
a. REPORT	**b. ABSTRACT**	**c. THIS PAGE**	Unlimited	6	Dr. Maxwell D. Gregoire
Unclassified	Unclassified	Unclassified			**19b. TELEPHONE NUMBER** *(include area code),*

Standard Form 298 (Rev. 8-98)
Prescribed by ANSI Std. 239.18

Noise measurements and current driver improvements for an atom interferometer gyroscope

M. M. Beydler, E. R. Moan, and C. A. Sackett
Department of Physics, University of Virginia, Charlottesville, Virginia 22904, USA

(Dated: October 8, 2023)

We present noise measurements for our Bragg interferometer gyroscope in a time-orbiting potential trap. We obtain an Allan deviation plot that demonstrates averaging improvement as $1/\sqrt{T}$ up to integration times T of 2.5 h. However, it exhibits an unexpected short term noise level of approximately 9 rad/$\sqrt{\text{Hz}}$. We attribute this primarily to real phase noise in the interferometer caused by fluctuations in the trap drive current. We have developed and constructed new high-bandwidth current amplifiers that we anticipate will improve performance.

I. NOISE MEASUREMENTS

The atom interferometer gyroscope described previously achieves a high level of sensitivity and stable operation, but exhibits short term phase noise. To better characterize this noise, we performed a standard Allan deviation measurement. We ran the experimental sequentially a total of 931 times, over a continuous period of 30 h. For each experimental run, we analyzed the output of each of two simultaneous interferometers. Output signals S_1 and S_2 were obtain as

$$S_i = \frac{N_{0i}}{N_{0i} + N_{+i} + N_{-i}}, \tag{1}$$

where N_{ji} is the number of atoms observed with final momentum $2j\hbar k$ in interferometer i. Ideally, we expect $S_i = S_{0i}[1 + V_i \cos(\xi \pm \Phi/2)]$, where $S_{0i} \approx 0.5$ is an offset, V_i is the visibility of the interferometer, ξ is a randomly varying phase, and Φ is the nominally constant Sagnac phase which encodes the rotation rate. One way to extract Φ is to plot S_2 vs. S_1, and in the absence of noise the points will fall on an ellipse

$$X^2 + Y^2 - 2XY\cos\Phi = \sin^2\Phi, \tag{2}$$

where $X \equiv (S_1/S_{10} - 1)/V_1$ and $Y \equiv (S_2/S_{20} - 1)/V_2$. Fitting the ellipse to this form yields Φ.

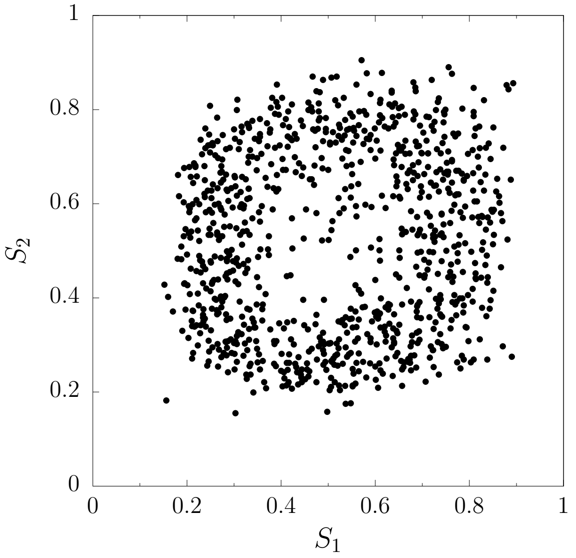

FIG. 1. Full data set for the Allen deviation experiment.

Figure 1 shows the results of all 931 experimental runs. The elliptical fit yields a value of $\Phi = 1.47(3)$ rad, but the data exhibit considerable scatter. To characterize the impact of the noise on the phase determination, we use the Allan deviation $\sigma(n)$, defined as the standard deviation of phase values obtained using data acquired in sequential sets of n runs. We calculated the Allan deviation by dividing the total data set into groups of $n \geq 10$ points, fitting each group to an ellipse, and calculating the standard deviation of the resulting phases. The results are shown in Fig. 2. The group size n can be converted to interrogation time T using the experimental cycle time of 80 s per run.

Two characteristics stand out in the the Allan deviation plot. First, $\sigma(n)$ averages down as $1/n^{1/2}$ all the way to $n = 100$, or $T = 8000$ s. This indicates that the apparatus exhibits no drifts on this time scale, which can be compared to typical drift times of 1 to 100 s for conventional rotation sensors such as ring laser gyroscopes, fiber optic gyros, or MEMS gyros. On the other hand, the overall scale of the noise is quite high. Extrapolating

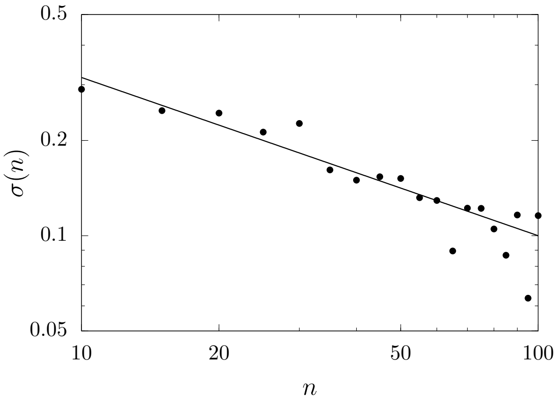

FIG. 2. Allan deviation results. The straight line shows the curve $1.0/\sqrt{n}$.

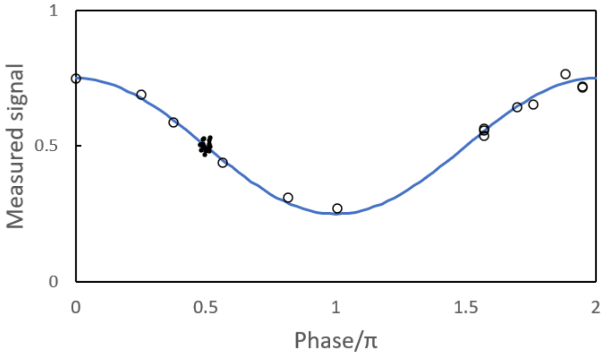

FIG. 3. Comparison of measurements for a conventional interferometer (solid black points) and a differential interferometer (open black points). The blue curve is the underlying signal as a function of phase.

back to $n = 1$ yields a total phase noise $\delta\Phi$ of 1 rad per run. The $1/n^{1/2}$ scaling in the Allan deviation indicates that this noise is uncorrelated between runs.

We can consider possible sources for this noise. Fundamentally, shot noise for our samples of approximately 10^4 atoms contributes phase noise of 0.01 rad, far below what we observe. Our detection system itself does not achieve shot noise limited performance, and the extra imaging noise corresponds optimally to $\delta\Phi = 0.03$ rad. We determined, however, that the ellipse fitting procedure does not achieve the standard shot noise or imaging noise limited performance, even in the absence of other noise sources. As illustrated in Fig. 3, a standard single interferometer measurement ideally uses measurements taken near the center of a sinusoidal fringe, where the sensitivity $dS/d\phi$ is maximal. In contrast, in a dual interferometer measurement of differential phase, data points are randomly acquired over the entire fringe, so many points provide less than optimal information. Numerical modeling indicates that for our level of imaging noise, the optimal phase precision is actually about 0.3 rad per run. The existence of this excess noise for differential phase measurements is not widely recognized, but will be significant for any precision measurement of this nature. The effect can be reduced by roughly a factor of two using a more sophisticated Bayesian analysis of the data.

Given that our measured phase noise of 1 rad is significantly larger than the estimated 0.3 rad measurement precision, we conclude that the apparatus is measuring a genuine noisy phase on the atoms. This is supported by numerical simulation, where adding both phase noise and imaging noise to the data results in a data set very similar to that observed in the experiment, including the 'squarish' shape compared to an ideal ellipse.

The only way to conclusively determine the source of this phase noise is to find the source and eliminate it. However, we can model the interferometer performance and look for likely culprits. We developed a semiclassical model for the evolution of wave packets in the interferometer, where the packets are assumed to follow a classical particle trajectory in the trap, and the packet phase evolves as the integral of the classical action $\phi = (1/\hbar)\int \mathcal{L}\,dt$, where $\mathcal{L}$ is the classical Lagrangian evaluated along the classical path. Ideally, in the absence of rotation the differential phase is zero, but we find that various types of experimental imperfections can result in nonzero Φ. We explored a large number of possible imperfections and calculated their effects on Φ up to third order. One simple contribution to the phase arises from an error $\Delta\omega$ in the trap frequency ω, in combination with a small xy contribution to the trapping potential, as

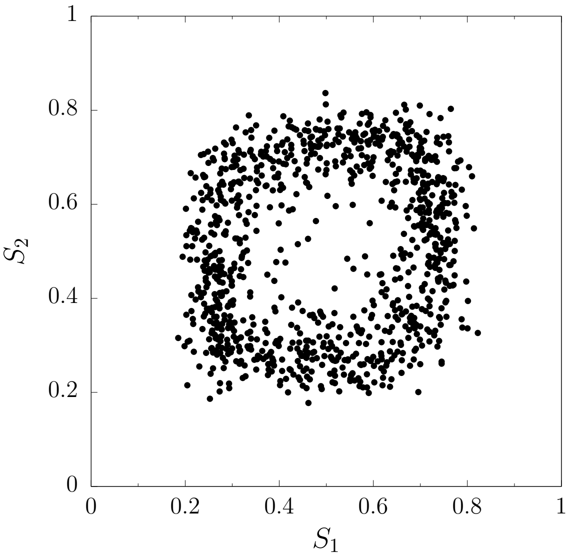

FIG. 4. Simulated data set including imaging noise with standard deviation 0.03 and phase noise with standard deviation 0.5 rad.

$$V(\mathbf{r}) = \frac{1}{2}m\omega^2(x^2 + y^2 + \zeta^2 z^2 + 2\gamma xy). \tag{3}$$

These errors give a differential phase contribution

$$\Delta\Phi = 2\pi^2 kR\gamma\frac{\Delta\omega}{\omega}, \tag{4}$$

where $k \approx 2\pi/(780\text{ nm})$ is the Bragg laser wave vector and $R \approx 0.57$ mm is the packet orbit radius. In the experiment, we estimate that γ is controlled to an accuracy of approximately 0.02. The trap frequency fluctuates from run to run due to noise in the current drivers, arising primarily from thermal variations in the coil resistance. We estimate this noise to give $\Delta\omega/\omega \approx 10^{-4}$. Together, these can be expected to produce run-to-run phase variations $\Delta\Phi \sim 0.2$ rad, which is on the order of the observed noise. Other phase noise contributors include angular misalignment of the Bragg beams, tilting of the trap potential with respect to gravity, and the relatively large fourth-order trap anharmonicity. In each case, the imperfect parameter couples to a fluctuation in the trap frequency to generate phase noise.

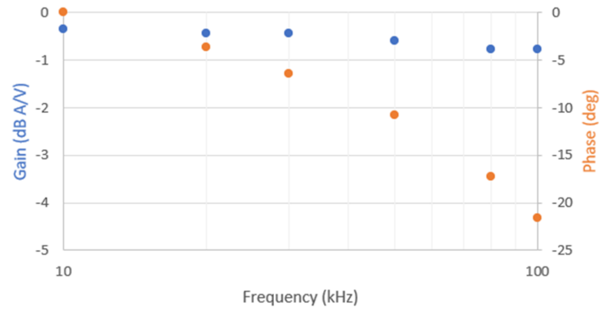

FIG. 5. Bode plot for the new current driver electronics.

II. CURRENT DRIVER IMPROVEMENTS

If the observed phase noise is caused by trap imperfections coupled to trap frequency fluctuations, then improving the trap frequency stability should reduce the phase noise. We believe that the trap instability is caused by thermal variations in the coil resistance. We use a feedback system in the current drivers to compensate for load variations, but the stabilization is not perfectly effective. Our TOP fields oscillate at frequency $\Omega = 2\pi \times 10$ kHz, and if the feedback system has bandwidth ω_f, then the noise reduction for a signal at Ω will be roughly Ω/ω_f. The drivers used for the data presented here have $\omega_f \approx 2\pi \times 100$ kHz, for a noise reduction factor of about 0.1.

As part of the A-PhI project, we developed and constructed improved current drivers with a bandwidth of 1 MHz. Here we do not have direct access to the open loop gain, but Fig. 5 shows that the closed-loop performance remains good up to 100 kHz frequencies. We tested the load sensitivity of the new driver by varying the temperature of the load coil. At a temperature variation of 110°, corresponding to a relative resistance variation of 0.37, we observe a relative current variation of -0.11. Over the full range of temperature, we observe $(R/I)dI/dR \approx -1/70$, roughly in line with expectations. Although a sufficient number of the new current drivers were not available before the end of the A-PhI project, we plan to test the interferometer performance with the new drivers and see if the observed phase noise decreases as expected.

The new current drivers offer several other advantages as well. The existing drivers rely on a tuned LC resonance circuit to negate the inductive load of the trap coils. This works well but it means that the operating frequency cannot be changed without altering the circuit. The new amplifiers do not rely on any resonance behavior and can operate freely over their full bandwidth. One application of this is to vary the TOP frequency Ω during the experiment. We require a relatively large value of Ω during evaporative cooling while the atoms are confined in a tight trap, but after adiabatic expansion into a weak trap for interferometry, Ω could be reduced by a factor of 10 or more. This would in turn improve the current stabilization proportionately.

Another application of the wideband drivers is to use more complex wave forms for the TOP fields. Currently the fields are sinusoidal, but by introducing additional frequency components at 2Ω, 3Ω, etc., it is possible to alter the anharmonic terms in the trap potential. This could also reduce the interferometer phase noise, since the noise effect depends a product of trap imperfections and current fluctuations. Through approaches such as these, we expect that several orders of magnitude improvement in the interferometer noise performance could be achieved.

DISTRIBUTION LIST

DTIC/OCP
8725 John J. Kingman Rd, Suite 0944
Ft Belvoir, VA 22060-6218 1 cy

AFRL/RVIL
Kirtland AFB, NM 87117-5776 1 cy

Official Record Copy
AFRL/RVB/Dr. Maxwell D. Gregoire 1 cy